CHEMISTRY
AN ASIAN JOURNAL

DOI: 10.1002/asia.201200526

Preparation of High-Performance Water-Soluble Quantum Dots for Biorecognition through Fluorescence Resonance Energy Transfer

Chin-Ping Huang,[b] Cheng-Fu Chao,[a] Mo-Yuan Shen,[a] Teng-Ming Chen,*[a] and Yaw-Kuen Li*[a]

Abstract: An improved method for the synthesis of high-performance and water-soluble quantum dots (QDs) involving the encapsulation of mercaptosuccinic acid coated QDs (MSA-QDs) with poly(diallyldimethylammonium chloride) (PDDA) followed by their direct photoactivation with fluorescent radiation near 295 K to yield PDDA-coated QDs (PDDA-QDs) has been demonstrated. The quantum yield (QY) of the PDDA-QDs was significantly improved from 0.6 (QY of MSA-QDs) to 48%. By using this synthetic strategy, highly photoluminescent PDDA-QDs of varied size were readily prepared. The surface properties of PDDA-QDs and MSA-QDs were extensively characterized. The highly luminescent and positively charged PDDA-QDs serve as a useful and convenient tool for protein adsorption. With a Δ^5-3-ketosteroid isomerase adsorbed PDDA-QD complex, the biorecognition of steroids was demonstrated through the application of fluorescent resonance energy transfer.

Keywords: FRET · molecular recognition · photoactivation · quantum dots · steroids

Introduction

The application of quantum dots (QDs) in life-science research is an active area of investigation. The demand for stable and highly luminescent water-soluble QDs has been strong. The existing methods for the synthesis of water-soluble QDs and related apparatus for bioapplications have common shortcomings, such as being tedious and expensive, involving complicated processing, and exhibiting weak luminescence.[1,2] Although a thiol reagent is the most common ligand used to stabilize QDs for potential biotechnical applications,[3–7] thiol-capped CdSe/ZnS QDs exhibit photochemical instability and low quantum yields (QYs) in solution. Many authors have reported that the stability of thiol-capped QDs, especially with semiconductor nanocrystals, was unsatisfactory, mainly because of the photooxidation of ligand/nanocrystal complexes[8–13] and the aggregation of particles.[8–9,11,13–14] This unstable nature prevents the reproducibility of nanocrystals for chemical and biochemical applications.

The investigation of photoactivation to enhance the photoluminescence of CdSe or CdSe/ZnS QDs in aqueous solution,[8,11,13–14] thin films,[15–19] and monolayers[20–24] has been discussed. After photoactivation, the spectral line for exciton photoluminescence (PL) of QDs is blueshifted, which indicates that the size of the QDs has decreased. This PL enhancement is attributed to ligand rearrangement on the QD surface that stabilizes the electron (or hole) traps. We report here an improved method that allows the synthesis of highly photoluminescent QDs with polymer encapsulation and photoactivation in consecutive processes. The general protocol for the synthesis of CdSe/ZnS QDs involves replacing hexadecylamine (HDA, a hydrophobic ligand) with D,L-mercaptosuccinic acid (MSA) and subsequent encapsulation with poly(diallyldimethylammonium chloride) (PDDA, a positively charged polymer) through electrostatic interaction.[25–27] These PDDA-encapsulated QDs then become subject to irradiation to form water-soluble, highly photoluminescent QDs, designated PDDA-QDs. The photoactivation improves the luminescent efficiency and decreases surface defects to minimize nonradiative recombination.[28] The encapsulated PDDA not only serves as a stabilizer to disperse QDs and to enhance the PL intensity but also functions as a matrix for adsorption of biomolecules. The properties of PDDA-QDs and MSA-QDs, such as surface charge, binding energy, and PL intensity, have been characterized and compared. We evaluate the feasibility of enzyme inhibition using Δ^5-3-ketosteroid isomerase (KSI)[29] and PDDA-QDs

[a] C.-F. Chao,[+] M.-Y. Shen, Prof. Dr. T.-M. Chen, Prof. Dr. Y.-K. Li
Department of Applied Chemistry
National Chiao Tung University
Science Building 2, 1001 Ta Hsueh Road
Hsinchu, Taiwan 300 (ROC)
Fax: (+886) 3-5723764
E-mail: ykl@faculty.nctu.edu.tw
tmchen@mail.nctu.edu.tw

[b] Dr. C.-P. Huang[+]
Nanotechnology Research Center
Nano-Instrumentation and Application Division
Industrial Technology Research Institute
195, Sec. 4, Chung Hsing Rd., Chutung
Hsinchu, Taiwan 31040 (ROC)

[+] These authors contributed equally to this work.

Supporting information for this article is available on the WWW under http://dx.doi.org/10.1002/asia.201200526.

to form a functional complex through fluorescent resonance energy transfer (FRET).

Results and Discussion

Optical Properties of Photoactivated PDDA-QDs

Previous investigations showed that molecular capping or photoactivation affects the PL intensity of QDs.[30–32] Water-soluble QDs are commonly synthesized through the replacement of their primary ligands, such as trioctylphosphine oxide (TOPO) or hexadecylamine (HDA), with thiol-containing agents. Poorly luminescent QYs are typically observed with nanoparticles prepared in this way.[6,8–10] Competition between nonradiative recombination of electron–hole pairs at the surface of thiol-coated QDs and band-edge emission is considered a possible mechanism to account for the small luminescence QY. Photoactivation that might involve the rearrangement of the surface structure and increase both the electron–hole pairs and the probability of radiative efficiency on the QD surface has been discussed.[8,9,11,13] Polymer capping, likely to eliminate the defects and traps on the QD surface, thereby yielding an increased electron–hole recombination, was demonstrated.[28] Our work on the preparation of highly luminescent water-soluble PDDA-QDs is based on these findings. The general protocol involves replacing the hydrophobic capping agent (e.g., HDA) with MSA and encapsulating the surface of the QDs with PDDA before photoactivation.

The luminescence of QDs was shown to be strongly affected by the capping agents.[33] Figure 1 shows the optical characterization of QDs with various capping molecules. Narrow emission lines centered at 562 (for MSA-QD) and 557 nm (for HDA-QD) were observed when QDs were excited with a He/Ne excitation source at 365 nm. The significantly decreased photoluminescence QY and the redshifted ($\approx$5 nm) features of the MSA-QDs are effects attributed to the trap states, which normally involve at least two processes. First, the hole is trapped with a thiol ligand such that radiative recombination of the exciton becomes impossible. Second, the redshifted exciton emission line might reflect an increasing delocalization of the wave function of the hole derived from newly accessible energy states on adsorbed chalcogenide atoms.[10,31] These drawbacks limit the potential of water-soluble, thiol-capped QDs for biological applications. In our work, the luminescence quantum yield of water-soluble QDs was greatly improved by using positively charged PDDA to coat the MSA-QDs followed by irradiation. Figure 1 shows the narrow emission line of PDDA-QDs centered at 533 nm under excitation at 365 nm. The emission intensity is clearly enhanced by 200-fold and the PL spectra are blueshifted ($\approx$29 nm) relative to that of MSA-QDs. After photoactivation, the PDDA-encapsulated MSA-QDs became highly luminescent (QY = 48 %), and the center of the PL spectrum was blueshifted from 562 to 533 nm, which indicated a decreased size of the QDs. The shrinkage might be due to photoetching,[11] and the photoenhancement likely resulted from the elimination of nonradiative recombination because the surface defects were passivated with PDDA. To compare the effect of polymer capping, poly(sodium styrenesulfonate) (PSS), a negative polyelectrolyte, was employed to cap the MSA-QDs. The effect of PSS on the PL intensity was insignificant; aggregation of QDs occurred after photoactivation. Figure 2 depicts the temporal evolution of the emission intensity of PDDA-QDs and demonstrates the temporal dependence of photoetching (or photoactivation) of the PDDA-QDs.

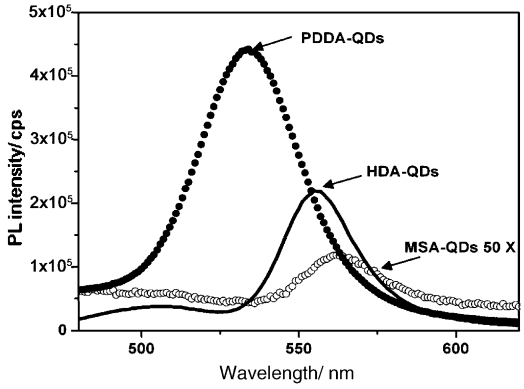

Figure 1. Comparison of PL spectra of X-QDs (X = HDA, MSA, and PDDA). Narrow emission bands centered at 557, 562, and 533 nm are observed with HDA-QD (——), MSA-QD (○), and PDDA-QD (●), respectively. Note that only PDDA-QDs were synthesized through a photoactivated process.

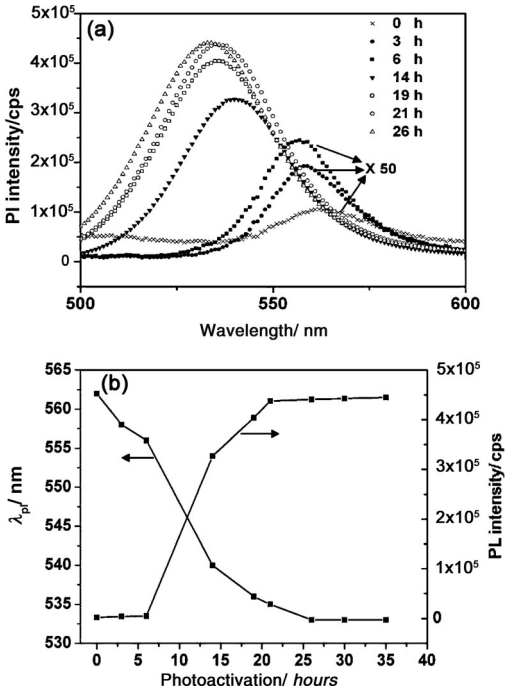

Figure 2. a) PL spectra of PDDA-QDs from time-dependent photoactivation. b) λ_{max} and PL intensity as a function of the photoactivation duration for PDDA-QDs.

In Figure 2a, the maximum emission line of the PDDA-QDs showed time-dependent blueshifting; the PL was progressively enhanced on photoactivation for 0 to 35 h. After phototreatment for 26 h, the QDs attained a stable stage with a maximal emission intensity and a maximally blueshifted emission line, as shown in Figure 2b. The PL was enhanced 200-fold and the maximum emission was blueshifted from 562 to 533 nm. The enhancement in the QY is attributed to increasing electrons and holes on the surface of the QDs and the increased probability of irradiative recombination, that is, surface-related emission.[13,19,21] The increased number of carriers (electrons and holes) at the QD surface is a direct consequence of the re-formation and optimization of the QD surface during photoactivation, which efficiently removes carrier quenching defects from the surface.[28] Photoactivation is thus employed not only to improve the QY but also to prepare QDs with varied size and emissions. Figure 3 shows the photoluminescence and images (inset) of

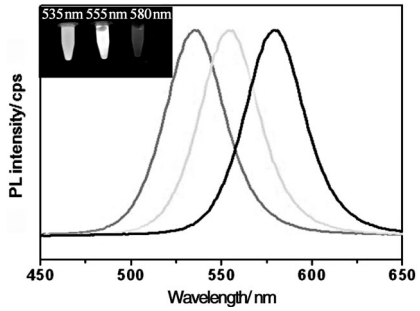

Figure 3. PL spectra of various PDDA-QDs. Emission peaks centered at 535 (left, QY = 48%), 555 (middle, QY = 43%), and 580 nm (right, QY = 20%) were observed when QDs were excited at 365 nm.

PDDA-QDs with the emission peaks centered at 535 (green, QY = 48%), 555 (yellow, QY = 43%), and 580 nm (red, QY = 20%) that were prepared by this method by starting with QDs exhibiting an emission maximum centered at (562 ± 5), (585 ± 5), and (609 ± 5) nm, respectively. These results show that the end products of various PDDA-QDs possess a narrow full width at half-maximum (FWHM, ≈36 nm) and a large QY.

Analysis of the Surface Charge and Size of PDDA-QDs

Migration in agarose gels is a convenient technique to verify the charge status of QDs.[34] Gel electrophoresis data showed that the MSA-QDs and PDDA-QDs migrated in opposite directions (Figure 1S in the Supporting Information), which is consistent with the predicted charge state on the QD surface. As a MSA-QD has a carboxylate group on its surface, it moved toward the positively charged electrode, whereas a PDDA-QD (with a positive charge on its surface) migrated to the negatively charged area. TEM allowed us to determine the distribution of the average size and the size of particles with varied capping agents.

Figure 4a–c shows PDDA-QDs of various sizes. The sizes of QDs with green, yellow, and red emission prepared from this method were found to be (3.2 ± 0.3), (3.5 ± 0.2), and (4.6 ± 0.2) nm, respectively. To identify the chemical process-

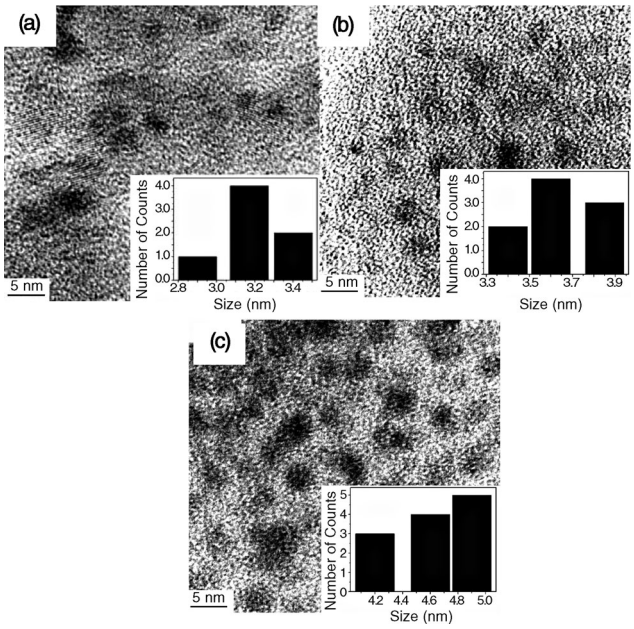

Figure 4. Size of various PDDA-QDs: a) green emission (λ_{max} = 535 nm), (3.2 ± 0.3) nm; b) yellow emission (λ_{max} = 555 nm), (3.5 ± 0.2) nm; and c) red emission (λ_{max} = 580 nm), (4.6 ± 0.2) nm.

es involved in photoactivation to achieve the PDDA-QDs, X-ray photoelectron spectroscopy (XPS) was used to analyze the composition of the final products. Multiple XPS measurements were recorded with MSA-QDs and PDDA-QDs. Typical survey spectra (Figure 2S in the Supporting Information), recorded in 10 min with an $Al_{K\alpha}$ source, presented these prominent signals from nanocrystals and surfaces: Cd $3d_{5/2}$, $3d_{3/2}$; Se 3d; Zn 3s; S 2p; C 1s; and O 1s. Table 1 summarizes the results and shows that the C 1s and O 1s signals of MSA-QDs and PDDA-QDs are likely from the capping layer of MSA and PDDA. Spectra in the regions of Cd and Se were examined at high resolution (Figure 5). For Cd and Se analysis, the binding energy from PDDA-QDs occurred at approximately 2 and 0.8 eV greater than those of MSA-QDs, respectively. The survey spectra (detailed data

Table 1. Core binding energy of component atoms of MSA-QDs and PDDA-QDs.

	Binding energy [eV]	
	MSA-QDs	PDDA-QDs
Se 3d	55.1	55.9
S 2p	161.5	163.2
C 1s	287.4	288.5
Cd $3d_{5/2}$	407	409
Cd $3d_{3/2}$	413.8	416
O 1s	533.1	534.8
Zn 3s	135	136.1

CHEMISTRY
AN ASIAN JOURNAL

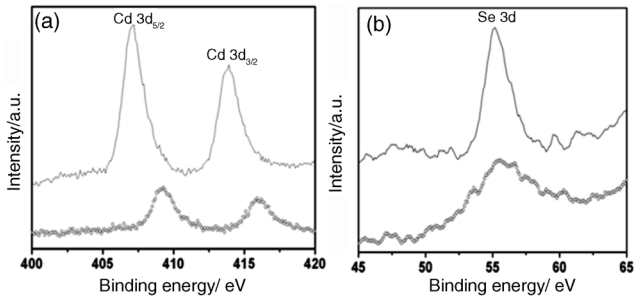

Figure 5. High-resolution XPS spectra of Cd and Se in QDs. a) Cd $3d_{5/2}$ at 407 eV (409 eV), Cd $3d_{3/2}$ at 413.8 eV (416 eV); b) Se 3d at 55.1 eV (55.9 eV) in MSA-QDs (——) and PDDA-QDs (–○–). Data shown in parentheses are for PDDA-QDs.

in Table 1) show that the binding energy shifted to increased energy and with decreased intensity. Possible explanations are that photoactivation dissolves the dangling bonds of the surface atoms and releases Cd, Se, Zn, and S ions to form the corresponding oxidized products and thereby perturb the binding energy of these measured elements, and that the PDDA capped on the MSA-QD surface might shelter the QDs from incident X-rays, thereby decreasing the intensity.

Demonstration of PDDA-QDs as a Biosensor through a FRET Quenching Assay

As the PDDA-QD possesses a highly charged surface for protein adsorption, it becomes a convenient tool for biorecognition through the application of FRET. To improve the performance of FRET, we prepared PDDA-QDs with a maximal emission wavelength of $\lambda_{max} = 543$ nm as the energy donor and tetramethylrhodamine-labeled cholic acid (TMR-CA) as the energy acceptor, with maximal absorption and emission at 560 and 580 nm, respectively (Figure 3S in the Supporting Information). The conditions of the binding assay are described in the Experimental Section (see below). The presence of TMR-CA with the KSI-absorbed PDDA-QDs (KSI/PDDA-QD) resulted in substantial fluorescence quenching at 543 nm but an emission band with $\lambda_{max} = 580$ nm through FRET. Figure 6 shows TMR-CA-dependent emission spectra, obtained from KSI/PDDA-QD (final concentration 0.495 μM) on mixing with various amounts of TMR-CA under excitation at 400 nm. At this wavelength, highly efficient excitation of PDDA-QD occurred, but TMR excitation was insignificant (Figure 4S in the Supporting Information). The enhancement in TMR fluorescence observed from the TMR-CA/KSI/PDDA-QD complex indicates that the FRET effect between PDDA-QDs and TMR was effective. The maximum quenching fluorescence of PDDA-QDs was observed when 0.89 μM TMR-CA (and above) was employed. The control experiment showed no significant quenching effect when PDDA-QDs were mixed with TMR-CA (up to 0.89 μM). The FRET efficiency $(1-r)$ can be calculated from the ratio (r) of the fluorescence intensities of the donor with acceptor divided by that without the acceptor. With TMR-CA = 0.89 μM, the FRET efficiency was estimated to be greater than 0.80.

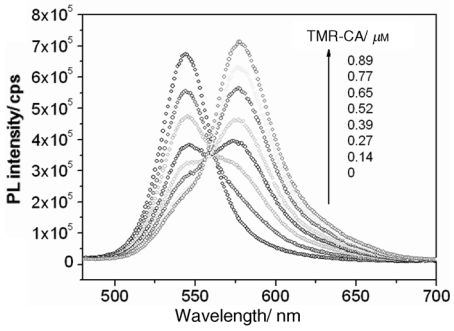

Figure 6. Emission spectra from KSI/PDDA-QD incubation with TMR-CA (various amounts from 0 to 0.89 μM). Samples were excited at 400 nm.

These results strongly indicate that KSI brought the two fluorophores together within the Förster distance to allow energy transfer to occur effectively between the donor and acceptor. We thus demonstrate that the FRET-based system using PDDA-QDs can achieve high sensitivity in monitoring biomolecular interactions. We further examined the feasibility of the application of the KSI/PDDA-QD complex for a KSI inhibition study through the reverse process of FRET. The sensing model was based on the competition between 4-estren-17β-ol-3-one (19NT) and TMR-CA to bind to KSI on PDDA-QD. The general protocol for this application is to mix the KSI/PDDA-QD complex with TMR-CA and 19NT at various concentrations; the FRET efficiency was monitored at the wavelength of maximal emission of PDDA-QD, namely, 543 nm.

Figure 7 presents a typical examination of the variation of the FRET efficiency at 543 nm with increasing concentration of the mixed solution (TMR-CA and 19NT). The results show a systematic recovery of the donor emission with increasing 19NT concentration, which indicates that 19NT competitively binds to KSI and consequently decreases the binding ratio of TMR-CA to KSI. Based on this sensing design, the study of biorecognition on KSI can be achieved, or a target analyte, such as 19NT, can be quantitatively determined by using the standard titration curve established by means of this system.

Conclusion

An improved method was developed to synthesize highly luminescent and water-soluble PDDA-QDs. The process involves polymer encapsulation and photoactivation with a fluorescent lamp. The PL intensity of PDDA-QDs was significantly enhanced at least 200-fold and was blueshifted 29 nm relative to MSA-QDs. This process is useful to synthesize QDs of varied sizes with an effective distribution and strong luminescence. The surface composition of PDDA-QDs was confirmed with XPS. PDDA-QDs possess a positively charged surface, which serves as a matrix for adsorption of

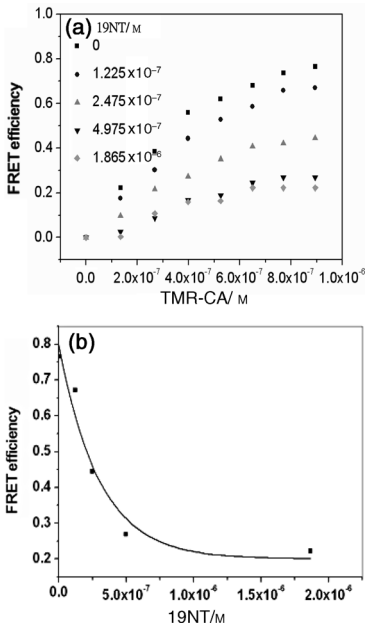

Figure 7. a)Variation of the FRET efficiency (at 543 nm) with mixed solutions (TMR-CA and 19NT) at various concentrations. FRET efficiency = $(I_0-I_f)/I_0$ (I_0 is the photoluminescent intensity of PDDA-QD; I_f is the photoluminescent intensity of PDDA-QD with TMR-CA and 19NT at various concentrations). b) Titration curve of the FRET efficiency (at 543 nm) with mixed solution (TMR-CA = 0.89 μM and various concentration of 19NT).

a protein (such as KSI). Through the application of FRET using a KSI/PDDA-QD complex, the interaction of cholic acid (or 19NT) with KSI can be addressed.

Experimental Section

Instruments and Chemicals

A UV-visible spectrophotometer (Hitachi U-3010A) and a spectrofluorimeter (Jobin–YvonSpex Fluolog-3) were used to investigate the fluorescence characteristics of the samples. All chemicals were analytical grade or the highest purity available. Chloroform, methanol, diethyl zinc (1 M solution in toluene), cadmium oxide, selenium, and sulfur powder (Aldrich); *n*-hexadecylamine (HDA) and stearic acid (SA) (Lancaster); tributylphosphine (TBP) (Showa); D,L-mercaptosuccinic acid (MSA), and tetramethylammonium hydroxide (TMAOH, 25 mass% in methanol) (Acros); and 4-estren-17β-ol-3-one (19NT) (Steraloids, Inc.) were acquired from the specified vendors. KSI was prepared according to the literature.[21] Tetramethylrhodamine-labeled cholic acid (TMR-CA) was synthesized on activating the carboxyl group on cholic acid with *N*-hydroxysuccinimide and treated with tetramethylrhodamine. The table lamp (Philips) had the specification of 21 W and intensity 8.5 mW cm^{-2} (for photoactivation).

Synthesis of PDDA-Capped CdSe/ZnS QDs through Photoactivation

Luminescent HDA-capped CdSe/ZnS QDs were synthesized as reported previously.[35,36] MSA was selected as the surface-capping agent to form water-soluble MSA-QDs. HDA-capped CdSe/ZnS QDs (30 mg) were dissolved in methanol (10 mL) and further transferred to a reaction vessel. A 1 M solution of MSA in methanol (50 mL) was added to the above solution; the pH value was adjusted to 11 with tetramethylammonium hydroxide pentahydrate. The mixture was kept in the dark and stirred at 30 °C overnight under N_2.[37] When the reaction was complete, the MSA-QDs were precipitated with methanol/propanone cosolvent (methanol/propanone (v/v) 5:2, 35 mL). MSA-QDs were collected by centrifugation ($4200 \times g$) and subsequently washed 10 times with methanol/propanone cosolvent (methanol/propanone (v/v) = 7:3, 10 mL). The MSA-QDs were then redissolved in a phosphate buffer (100 mM, pH 8.0). MSA-QD solution (1 mL, 1 OD) was added dropwise into the PDDA solution (0.5 mL, 17.8 mg mL^{-1} in deionized water) that was prepared in a 5 mL glass vial. The resulting solution was ultrasonicated for 10 min before photoactivation. For carrying out photoactivation, the glass vial was placed horizontally and about 10 cm beneath a Philips table lamp (21 W, intensity 8.5 mW cm^{-2}) for 24 h at 295 K. The highly photoluminescent PDDA-QDs were further obtained on centrifugation ($10\,600 \times g$) for 10 min and were redissolved in deionized water.

Analysis of Surface Charge and Size of PDDA-QDs

For analysis of the surface charge of QDs, we performed electrophoresis with agarose gel (0.5%). Gels were prepared in TAE buffer (0.4 M tris(hydroxymethyl)aminomethane (Tris), 0.01 M ethylenediaminetetraacetate (EDTA), 1.142% acetic acid, pH 10.0). For TEM, a microscope (Philips TECNAI 20) was operated at 200 kV. The samples were prepared by dropping diluted solutions of PDDA-QD nanocrystals onto 200 mesh carbon-coated copper grids. Samples of MSA-QD and PDDA-QD for XPS were prepared by depositing the corresponding sample solution onto a wafer, which was then kept in darkness; the solvent was removed with nitrogen. XPS spectra were recorded on a spectrometer (VG Scientific, Microlab 350) with $Al_{K\alpha}$ radiation.

Preparation of PDDA-QDs for Biorecognition

KSI solution (20 μL, 29.9 μM) and PDDA-QDs (10 μL, 9.9 μM) were mixed and incubated for 1 h at 4 °C in the dark. A phosphate buffer solution (20 mM, pH 7.5) was added to each tube (final volume 120 μL). Various amounts (0–70 μL) of TMR-CA (2.55 μM; concentration calculated with $\varepsilon = 65\,000$ cm^{-1} M^{-1} at 550 nm) were added to the above solution; the mixture was incubated at 4 °C for 15 min. A phosphate buffer solution (20 mM, pH 7.5) was added (final volume 200 μL). The resulting mixtures were then placed in a cuvette (path length 1 cm) for photoluminescence measurement. For a KSI inhibitor competition assay, the same amount of KSI and PDDA-QDs were mixed and incubated for 1 h at 4 °C in the dark. To the solution, various amounts of TMR-CA (0–0.894 μM) and 19NT (0–1.865 μM) were added; the mixture was then incubated at 4 °C for 15 min. The pH of the mixture was further adjusted by adding phosphate buffer solution (20 mM, pH 7.5, final volume 200 μL) for measurement of photoluminescence.

Acknowledgements

The authors are grateful to the National Science Council of Taiwan for financial support.

[1] M. Wang, M. Zhang, J. Qian, F. Zhao, L. Shen, G. D. Scholes, M. A. Winnik, *Langmuir* **2009**, *25*, 11732–11740.
[2] Y. J. Bao, J. J. Li, Y. T. Wang, L. Yu, J. Wang, W. J. Du, L. Lou, Z. Q. Zhu, H. Peng, J. Z. Zhu, *Opt. Mater.* **2012**, *34*, 1588–1592.
[3] Z. Zhelev, R. Bakalova, H. Ohba, R. Jose, Y. Imai, Y. Baba, *Anal. Chem.* **2006**, *78*, 321–330.
[4] W. Liu, H. S. Choi, J. P. Zimmer, E. Tanaka, J. V. Frangioni, M. Bawendi, *J. Am. Chem. Soc.* **2007**, *129*, 14530–14531.
[5] C. A. Constantine, K. M. Gattás-Asfura, S. V. Mello, G. Crespo, V. Rastogi, T.-C. Cheng, J. J. DeFrank, R. M. Leblanc, *J. Phys. Chem. B* **2003**, *107*, 13762–13764.
[6] X. Ji, J. Zheng, J. Xu, V. K. Rastogi, T.-C. Cheng, J. J. DeFrank, R. M. Leblanc, *J. Phys. Chem. B* **2005**, *109*, 3793–3799.
[7] J. J. Zheng, F. M. Gao, G. D. Wei, W. Y. Yang, *Chem. Phys. Lett.* **2012**, *519–520*, 73–79.

[8] C. Carrillo-Carrión, S. Cárdenas, B. M. Simonet, M. Valcárcel, *Chem. Commun.* **2009**, 5214–5226.
[9] J. A. Kloepfer, S. E. Bradforth, J. L. Nadeau, *J. Phys. Chem. B* **2005**, *109*, 9996–10003.
[10] S. F. Wuister, C. M. Donegá, A. Meijerink, *J. Phys. Chem. B* **2004**, *108*, 17393–17397.
[11] T. Torimoto, S. Murakami, M. Sakuraoka, K. Iwasaki, K. Okazaki, T. Shibayama, B. Ohtani, *J. Phys. Chem. B* **2006**, *110*, 13314–13318.
[12] M. Jones, J. Nedeljkovic, R. J. Ellingson, A. J. Nozik, G. Rumbles, *J. Phys. Chem. B* **2003**, *107*, 11346–11352.
[13] J. Aldana, Y. A. Wang, X. Peng, *J. Am. Chem. Soc.* **2001**, *123*, 8844–8850.
[14] I. Costas-Mora, V. Romero, F. Pena-Pereira, I. Lavilla, C. Bendicho, *Anal. Chem.* **2011**, *83*, 2388–2393.
[15] H. Fujiwara, H. Ohta, T. Chibaa, K. Sasakia, *J. Photochem. Photobiol. A* **2011**, *221*, 160–163.
[16] Y. Wang, Z. Tang, M. A. Correa-Duarte, I. Pastoriza-Santos, M. Giersig, N. A. Kotov, L. M. Liz-Marzán, *J. Phys. Chem. B* **2004**, *108*, 15461–15469.
[17] Y. Wang, Z. Tang, M. A. Correa-Duarte, L. M. Liz-Marzán, N. A. Kotov, *J. Am. Chem. Soc.* **2003**, *125*, 2830–2831.
[18] G. Crivat, S. M. Da Silva, D. R. Reyes, L. E. Locascio, M. Gaitan, N. Rosenzweig, Z. Rosenzweig, *J. Am. Chem. Soc.* **2010**, *132*, 1460–1461.
[19] A. Y. Nazzal, X. Wang, L. Qu, W. Yu, Y. Wang, X. Peng, M. Xiao, *J. Phys. Chem. B* **2004**, *108*, 5507–5515.
[20] M. Mitsuishi, S. Morita, K. Tawa, J. Nishii, T. Miyashita, *Langmuir* **2012**, *28*, 2313–2317.
[21] T. Uematsu, S. Maenosono, Y. Yamaguchi, *J. Phys. Chem. B* **2005**, *109*, 8613–8618.
[22] S. R. Cordero, P. J. Carson, R. A. Estabrook, G. F. Strouse, S. K. Buratto, *J. Phys. Chem. B* **2000**, *104*, 12137–12142.
[23] J. Xu, C. Wang, R. M. Leblanc, *Colloids Surf. B* **2009**, *70*, 163–170.
[24] E. M. Likovich, R. Jaramillo, K. J. Russell, S. Ramanathan, V. Narayanamurti, *Adv. Mater.* **2011**, *23*, 4521–4525.
[25] G. Jie, L. Li, C. Chen, J. Xuan, J. J. Zhu, *Biosens. Bioelectron.* **2009**, *24*, 3352–3358.
[26] F. Yang, Q. Ma, W. Yu, X. Su, *Talanta* **2011**, *84*, 411–415.
[27] Q. Ma, E. Ha, F. Yang, X. Su, *Anal. Chim. Acta* **2011**, *701*, 60–65.
[28] S. Zhang, J. Yu, X. Li, W. Tian, *Nanotechnology* **2004**, *15*, 1108–1112.
[29] K. S. Chang, C. C. Chen, J. T. Sheu, Y.-K. Li, *Sens. Actuators B* **2009**, *138*, 148–153.
[30] X. Wang, L. Qu, J. Zhang, X. Peng, M. Xiao, *Nano Lett.* **2003**, *3*, 1103–1106.
[31] N. Myung, Y. Bae, A. J. Bard, *Nano Lett.* **2003**, *3*, 747–749.
[32] C. Luccardini, C. Tribet, F. Vial, V. Marchi-Artzner, M. Dahan, *Langmuir* **2006**, *22*, 2304–2310.
[33] C. Bullen, P. Mulvaney, *Langmuir* **2006**, *22*, 3007–3013.
[34] T. Pellegrino, L. Manna, S. Kudera, T. Liedl, D. Koktysh, A. L. Rogach, S. Keller, J. Rädler, G. Natile, W. J. Parak, *Nano Lett.* **2004**, *4*, 703–707.
[35] G. W. Huang, C. Y. Chen, K. C. Wu, M. O. Ahmed, P. T. Chou, *J. Cryst. Growth* **2004**, *265*, 250–259.
[36] D. V. Talapin, A. L. Rogach, A. Kornowski, M. Haase, H. Weller, *Nano Lett.* **2001**, *1*, 207–211.
[37] C. P. Huang, Y. K. Li, T. M. Chen, *Biosens. Bioelectron.* **2007**, *22*, 1835–1838.

Received: June 12, 2012
Revised: August 20, 2012
Published online: September 25, 2012

